



Adsorption Efficiency of Nano/Micro Cellulose for Removing Iron from Aqueous Solution and its Isotherm Studies

Harendra Kumar Sharma^{1*}, Manoharmayum Vishwanath Sharma¹, Rabia Quadir¹ and Laxmi Dubey²

¹School of Studies in Environmental Science, Jiwaji University, India

²S.M.S. Govt. Model Science College, Gwalior, India

Corresponding author email: drsharmahk@yahoo.com

ABSTRACT

The increasing industrial activity and the influx of the heavy metal contaminated water into the environment has become a major concern in the developing countries. This also bring along with it the concern of severe health related issue due to the toxicity of the heavy metal and their non-degradable nature. Moreover they can be mutagenic and carcinogenic and are difficult in treatment by chemical as well as biological means. Iron even though is required for metabolism but it in excess it is more harmful. The study is focused on the synthesis of Nano/Micro cellulose and its application in the removal of iron from aqueous solution. The synthesized Nano/Micro Cellulose was characterized with techniques such as Particle Size Analyzer (PSA), Powder X-Ray Diffraction, and Fourier Transformation Infra-Red Spectroscopy (FTIR). The characterization indicated that the material is crystalline in nature and that the material was in Nano/Micro meter range. The material was then tested for its ability to remove iron from aqueous solution and the Freundlich, Langmuir and Temkin isotherm model were tested. The material showed ability of iron removal of 93.8% and Langmuir isotherm being the most suitable in this case.

Keywords: Heavy metal, Cellulose, Characterization, Iron, Removal, Isotherm

Received 02.10.2020

Revised 27.12.2020

Accepted 03.02. 2021

INTRODUCTION

Developing countries are facing a major concern of heavy metal pollution which include discharge of heavy metal contaminated water. This may affect the water quality and may lead to severe health related issues due to their toxicity and non-degradability[1]. The high persistence, damage to the nervous system, mutagenic and carcinogenic due to accumulation of the heavy metals on top of the difficulty in treatment of the contaminated sites by chemical or biological means has drawn much attention [2-3]. Considering the rapidly growing population, the increasing water scarcity issues and the non-degradability, the water consumption pattern is needed to be reconsidered [3].

The presence of iron in excess can be toxic even though it is required for plant metabolism. The influx of waste water contaminated with heavy metals in the environment with the increasing industrial activities has become a major issue [4]. Iron is commonly found in the effluents of many industry and techniques for the removal mainly include but not limited to chemical precipitation, ion exchange, electrochemical treatment, crystallization and membrane process [5]. More economical and ecofriendly methods using biomass of both plant or animal origin, waste materials, coir fiber, wooden charcoal and pine bark have also been investigated [6-20].

MATERIAL AND METHODS

Synthesis of Nano/Micro Cellulose

Nano/Micro Cellulose was synthesized through a two-step acid hydrolysis. Whattmann filter paper no.1 was used as the source of cellulose. The Whattmann filter paper was first cut into small pieces and added to a 45% H₂SO₄. Upon the dispersion of the cellulose fiber into the acid solution the dispersed and partially hydrolyzed cellulose fibers were then again transferred to 60% H₂SO₄. It was seen that if the Whattmann filter paper pieces were added to 60% H₂SO₄ directly then it led to the blackening of the cellulose indicating carbonization of the cellulose fibers. This was avoided by treatment of the cellulose material with 45% H₂SO₄ first followed by 60% H₂SO₄. The cellulose in acid solution is then sonicated for 1 hour and left undisturbed for 5 days.

Characterization

The characterization of prepared Nano/Micro Cellulose was done at Central Instrumentation Facility of Jiwaji University, India. The X-Ray Diffraction analysis was done with the help of Rigaku (Modal no Mini Flex 600). Perkin Elmer Modal no. Spectrum Two Serial no. 105627 FT-IR was used for Fourier Transformation Infrared Spectroscopy done.

Estimation of Iron

Total iron is the sum of both the ferric and ferrous iron concentrations. The combination of the ferric ions with thiocyanate ions results in the formation of red coloured ferric thiocyanate which has been measured colorimetrically. Iron estimation was carried out by spectrophotometric method using thiocyanate method [21]. The absorbance of the dark red colour complex formed was studied at 490nm. Absorbance of known standard samples was recorded and graph of absorption versus concentration of iron (ppm) was plotted.

Batch mode adsorption studies

Batch mode adsorption studies for individual metal compounds were carried out to investigate the effect of different parameters such as adsorbate concentration, adsorbent dosage, agitation time and pH. The solution (100mL) containing adsorbate and adsorbent was taken in 250ml conical flasks and agitated in a mechanical shaker at predetermined time intervals. The adsorbate was separated from the adsorbent using filter paper. The range of different parameters studied by various adsorbents in the present work is given in Table 1.

Table no.1. Range of different parameters investigated for the adsorbents

Parameters	Values Investigated
Agitation time (min)	30, 45, 60,75 and 90
Adsorbent dosage, (gm)	0.07, 0.14, 0.21, 0.28, 0.35, 0.42 and 0.56
Initial concentration, C _i , mg/L	15, 20, 25, 30, 50, 70, 100, 130

The effect of change in pH could not be studied as precipitation kept forming whenever attempts were made to adjust the pH for the study.

RESULTS

PSA

The Particle Size Analysis of the material indicated that the size of the material ranged from 147 nanometer to 1781.5 micrometer (Fig. 1). The particle size analyzer considers particle agglomeration as a single particle and the size of the material is given in diameters. So the particle size analyzer cannot give an exact value of the size but only an estimate of the size.

XRD

The Powder X-Ray Diffraction analysis of the material showed that the peaks prominent at angles $2\theta = 17^\circ$, 21.88° , 33.62° and 45.44° (Fig 2). The calculated of the crystallite size was done using the Scherrer's formula and was found to be 0.79 nm [22].

$$\text{Scherrer's formula, } \tau = \frac{K\lambda}{\beta \cos\theta}$$

Where τ is the crystallite size, K is a crystallite shape factor, λ is the wavelength of X-ray, β is the full width at half maximum of the X-ray diffraction peak and θ is the Bragg angle.

FTIR

FTIR was performed to determine functional groups of the synthesized Nano/Micro Cellulose. The FTIR spectra synthesized Nano/Micro Cellulose (Fig. 3) indicated peaks at 3400, 2909, 2138, 1643 and 1430 are associated with the adsorbent. The peak at 3400 cm^{-1} , is due to O-H stretching and 2909 cm^{-1} is due to C-H stretching and 2138 cm^{-1} is due to $\text{C}\equiv\text{C}$ Stretch and 1643 cm^{-1} is due alkene stretch.

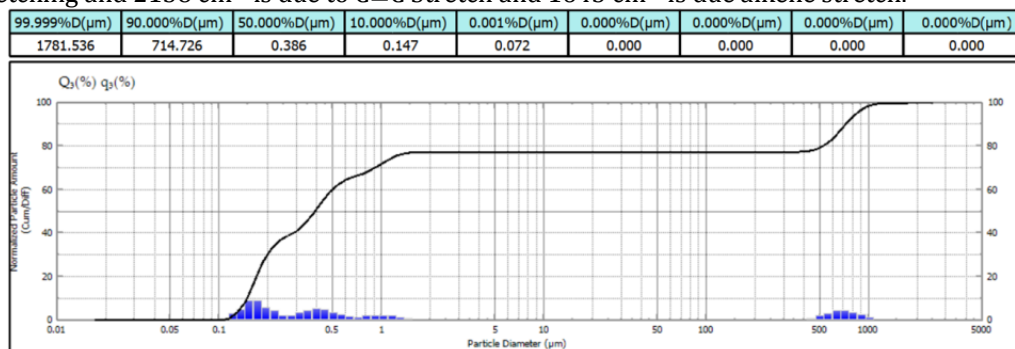


Fig 1. PSA of the synthesized Nano/Micro Cellulose

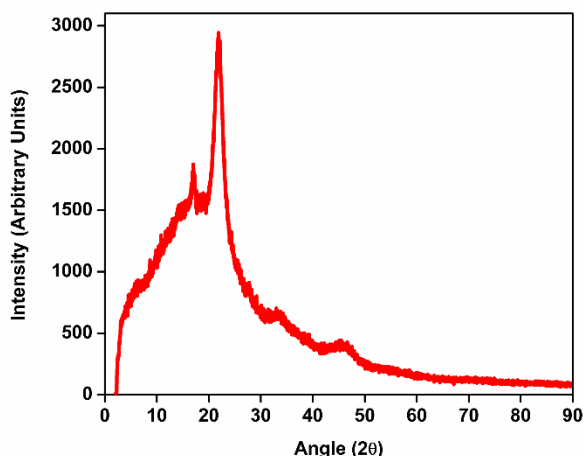


Fig 2. Powder XRD of the synthesized Nano/Micro Cellulose

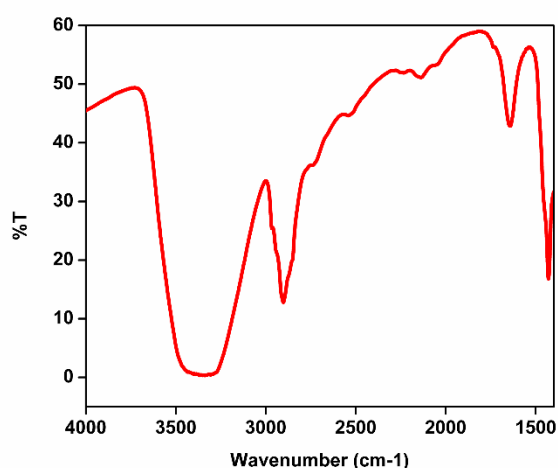


Fig 3. FTIR of the synthesized Nano/Micro Cellulose

Effect of Contact time

The adsorption of iron onto Nano/Micro Cellulose as a function of contact time is shown in Fig 4. The experiments were carried out at different contact times varying from 30 to 90 min, with adsorbent dose (0.14g), initial concentration (10mg/L) at a pH 2 and 100 ml contact solution. The percentage removal of iron is depicted in Fig 4. As the contact time was changed from 30 to 90 minutes, removal gradually increased from 30 to 60 minutes and then it starts decreasing. The maximum removal of 22.5% was obtained at 60 minutes and afterwards removal efficiency decreased. It may be noted that initially, the adsorption is more and it slows down with time and reaches a steady state after a certain time and the removal efficiency almost remains constant. This is due to the fact that initially, more number of active sites are available for the fruitful adsorption of Iron, and as the sites are progressively used up with time, the rate of adsorption is slow down. As the contact time increased the active sites on the sorbent were filled. Furthermore, by increasing the contact time after attaining the equilibrium may result in detachment of iron from adsorbent and hence results in decrease in removal percentage[23].

Effect of Concentration

This parameter provides an important aspect to overcome all mass transfer resistance of the metal between aqueous solution and adsorbent phase. The experiments were done with variable iron concentration varying from 15ppm to 130ppm, and the other parameters like dose, contact time and pH were taken as constant. It is evident from the Fig. 5 that by increasing initial iron concentration; removal efficiency was also increased and remained nearly constant after equilibrium time. The maximum removal percentage of 83.8% was achieved at 50 ppm. It can be seen from the figure no. 33 that the percentage removal decreases with the increase in metal ion concentration. At lower initial metal ion concentrations, a lot of adsorption sites are available for adsorption of the heavy metals ions. Though, at

high concentration the available sites of adsorption become fewer and hence the removal percentage of heavy metal is dependent upon the metal ion concentration [23].

Effect of Dose

It is an important parameter as it determines the capacity of adsorbent to remove metal from the solution. The dependence of Iron sorption on dose was studied by varying the amount of adsorbents of Nano/Micro Cellulose from 0.07g to 0.63g, while keeping other parameters contact time, metal ion concentration constant. The results for removal of iron with respect to adsorbent dose are shown in Fig. 6. It is shown that there is a sharp increase in percentage removal with increasing adsorbent dose. The highest uptake was obtained at bioadsorbent concentration of 0.49g with the removal of 93.8%. The removal of metal ions increased with the increase in biosorbent concentration and equilibrium was attained after 0.49g of adsorbent dosage for the Iron ions. This is attributed due to availability of more biosorbent sites as well as enhanced surface area [23]. The decrease in the rate of Iron uptake at adsorbent dose greater than 0.49g may be due to competition of the metal ion for the sites available.

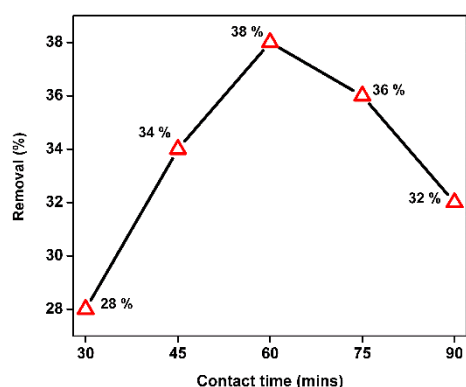


Fig 4. Effect of Contact Time

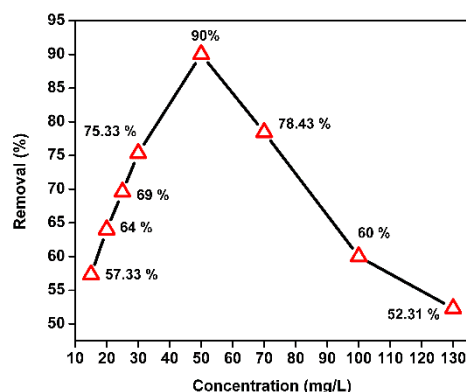


Fig 5. Effect of Concentration

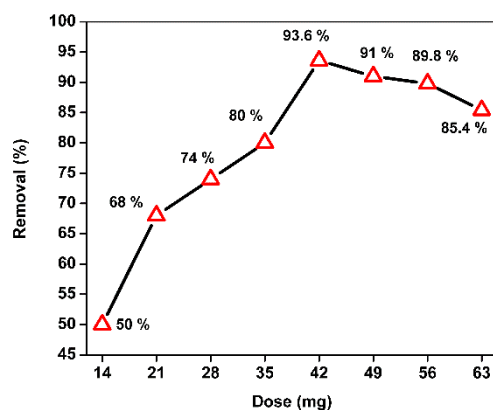


Fig 6. Effect of Dose Time

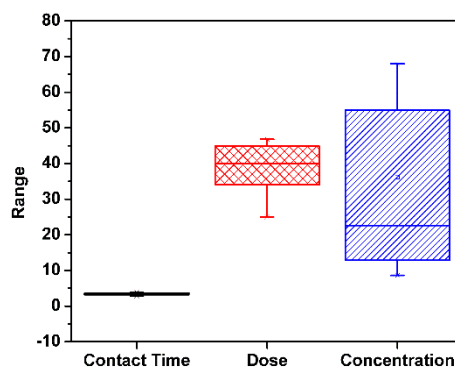


Fig.7 Effect of different parameters

Effect of Different Parameters

The effect of different parameters have been compared by plotting a box plot of the changes in the concentration after optimization of each parameter (Fig. 7). The graph showed that change in the metal concentration has the highest effect in the study, followed by dose of the adsorbent and then the contact time. This indicates that the concentration of the metal ions plays a major role in optimum and effective removal of the metal ions from the aqueous solution.

Isotherms

The data of equilibrium for the adsorption are commonly known as adsorption isotherms. It is essential to know them so as to compare the effectiveness of different adsorbent materials under different operational conditions and also to design and optimize an adsorption system. Heavy metal adsorption is usually modelled by the classical adsorption isotherms. In this study, three isotherms models were used, Langmuir, Freundlich and Temkin isotherms[24-26].

The homogeneity of the surface, the energy of the active sites and the active site distribution and the enthalpy change logarithmically forms the basis of Freundlich isotherm model.

The equation of Freundlich isotherm is:

$$q_e = K_F C_e^{1/n}$$

Where q_e = amount of dye degraded per unit mass of nanomaterials (mg/g), C_e = equilibrium concentration (mg/L), K_F and n are freundlich equilibrium constants.

The Langmuir Isotherm is widely used and has been applied in degradation and adsorption processed.

The equation of the Langmuir isotherm is:

$$q_e = \frac{q_m K_L C_e}{1 + K_L C_e}$$

Where C_e = equilibrium concentration, K_L = the relative energy of degradation (L/mg) and q_m = Langmuir constants related to maximum degradation capacity (mg/g).

The Temkin Isotherm model assumes a linear decrease in the heat of adsorption of all molecules in the layer with the consideration of adsorbent-adsorbate interaction.

The equation of the Temkin isotherm is

$$q_e = B \ln A_T + B \ln C_e$$

Where B =Constant related to heat of sorption (J/mol) and A_T = Temkin isotherm equilibrium binding constant (L/g).

For Freundlich isotherm a graph of $\log C_e$ was plotted against $\log q_e$ (Fig. 8), C_e/q_e against C_e for Landmuir isotherm (Fig. 9) and q_e against $\ln C_e$ for Temkin isotherm (Fig. 10). The isotherm data has been given below in Table 2.

The calculated values of correlation coefficient (R^2), n and K_f for the Freundlich isotherm are 0.718, 4.34783 and 7.8886 (mg/g) respectively, for Langmuir isotherm the value of R^2 , q_m and K_L are 0.923, 20.8333 (mg/g) and 0.18321 (L/mg) respectively and for Temkin isotherm the value of R^2 , B and A_T are 0.698, 3.211 (J/mol) and 6.991 (L/g) respectively. The correlation coefficient value R^2 of the three isotherm indicates that Langmuir isotherm model is best suited in this study.

Table 2. Isotherm constants
Freundlich Isotherm

K_f	n	R^2
7.8886	4.34783	0.718
Langmuir Isotherm		
K_L	q_m	R^2
0.18321	20.8333	0.923
Temkin Isotherm		
A_T	B	R^2
6.991	3.211	0.698

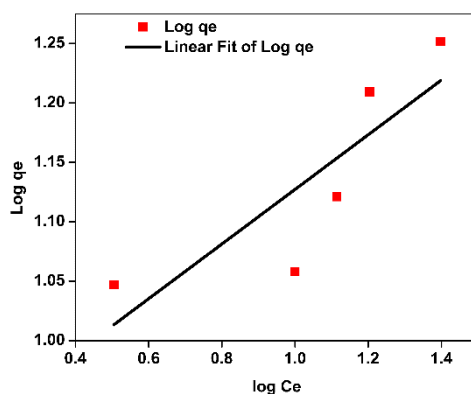


Fig 8. Freundlich Isotherm

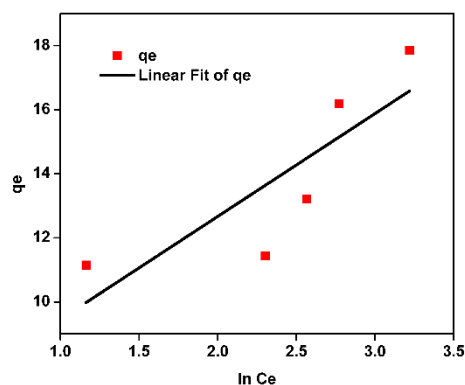
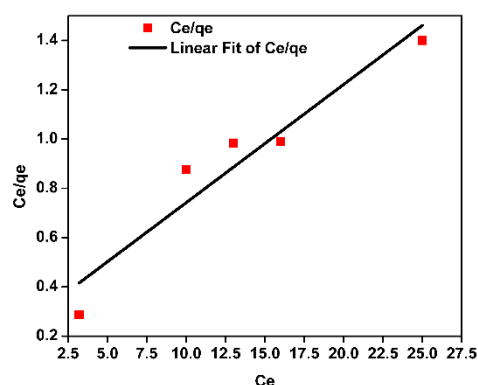


Fig 9. Langmuir Isotherm

Fig 10. Temkin Isotherm

CONCLUSION

Cellulose is one of the most abundant materials. It is environmentally friendly and has the viability for becoming a widely used biopolymer material. The study explores environmental application of Nano/Micro Cellulose through its use in removal of iron from aqueous solution. The different parameters effecting the removal of iron from aqueous solution were studied and optimized to analyze the maximum removal potential. pH as a parameter could not be studied with the same method as the precipitate formation was seen whenever the pH was adjusted. The study revealed that Nano/ Micro Cellulose is a viable material for the removal of iron and has the potential of above 93% removal of iron from solution. The application of this ecofriendly material can be explored for various other applications.

ACKNOWLEDGEMENTS

The authors are thankful to Jiwaji University, Gwalior for assistance and support of innovative research and development. The authors also extend their gratitude to Central Instrumentation Facility, Jiwaji University for the providing instrumentation facilities.

CONFLICT OF INTERESTS

The authors have no conflict of interest of any manner.

REFERENCES

1. N. D. Tumin, A. L. Chuah, Z. Zawani, and S. A. Rashid, (2008). "Adsorption of copper from aqueous solution by Elais Guineensis kernel activated carbon," *J. Eng. Sci. Technol.*, vol. 3, no. 2, pp. 180–189.
2. R. Goyer, (2011). *The Basic Science of Poisons*, 4th ed. New York: Pergamon Press.
3. M.-H. Yu, (2016). *Environmental Toxicology: Biological and Health Effects of Pollutants, Third Edition*, 3rd ed. CRC Press.
4. K. C. Sekhar, C. T. Kamala, N. S. Chary, and Y. Anjaneyulu, (2003). "Removal of heavy metals using a plant biomass with reference to environmental control," *Int. J. Miner. Process.*, vol. 68, no. 1–4, pp. 37–45.
5. S. Babel and T. A. Kurniawan, (2003). "Low-cost adsorbents for heavy metals uptake from contaminated water: a review," *J. Hazard. Mater.*, vol. 97, no. 1–3, pp. 219–243.

6. R. Razmovski and M. Šciban, (2008). "Iron (III) biosorption by *Polyporus squamosus*," *Afr. J. Biotechnol.*, vol. 7, no. 11, 20-28.
7. A. García-Mendieta, M. T. Olguín, and M. Solache-Ríos, (2012). "Biosorption properties of green tomato husk (*Physalis philadelphica* Lam) for iron, manganese and iron-manganese from aqueous systems," *Desalination*, vol. 284, pp. 167-174.
8. N. T. Abdel-Ghani, A. K. Hegazy, G. A. El-Chaghaby, and E. C. Lima, (2009). "Factorial experimental design for biosorption of iron and zinc using *Typha domingensis* phytomass," *Desalination*, vol. 249, no. 1, pp. 343-347.
9. [9] M. Tuzen, O. D. Uluozlu, C. Usta, and M. Soylak, (2007). "Biosorption of copper (II), lead (II), iron (III) and cobalt (II) on *Bacillus sphaericus*-loaded Diaion SP-850 resin," *Anal. Chim. Acta*, vol. 581, no. 2, pp. 241-246.
10. A. Selatnia, A. Boukazoula, N. Kechid, M. Z. Bakhti, A. Chergui, and Y. Kerchich, (2004). "Biosorption of lead (II) from aqueous solution by a bacterial dead *Streptomyces rimosus* biomass," *Biochem. Eng. J.*, vol. 19, no. 2, pp. 127-135.
11. M. Aryal, M. Ziajova, and M. Liakopoulou-Kyriakides, (2010). "Study on arsenic biosorption using Fe (III)-treated biomass of *Staphylococcus xylosus*," *Chem. Eng. J.*, vol. 162, no. 1, pp. 178-185.
12. Y. Sağ and T. Kutsal, (1998). "The simultaneous biosorption of Cr (VI), Fe (III) and Cu (II) on *Rhizopus arrhizus*," *Process Biochem.*, vol. 33, no. 5, pp. 571-579.
13. V. Lugo-Lugo, C. Barrera-Díaz, F. Ureña-Núñez, B. Bilyeu, and I. Linares-Hernández, (2012). "Biosorption of Cr (III) and Fe (III) in single and binary systems onto pretreated orange peel," *J. Environ. Manage.*, vol. 112, pp. 120-12.
14. Z. Aksu and Ü. Açikel, (2000). "Modelling of a single-staged bioseparation process for simultaneous removal of iron (III) and chromium (VI) by using *Chlorella vulgaris*," *Biochem. Eng. J.*, vol. 4, no. 3, pp. 229-238.
15. A. Saravanan, V. Brindha, E. Manivannan, and S. Krishnan, (2010). "Kinetics and isotherm studies of mercury and iron biosorption using *Sargassum* sp," *Int J Chem Sci Appl*, vol. 1, no. 2, pp. 50-60.
16. K. K. P. Porpino, M. da C. S. Barreto, K. B. Cambuim, J. R. de Carvalho Filho, I. A. S. Toscano, and M. de A. Lima, (2011). "Fe (II) adsorption on *Ucides Cordatus* crab shells," *Quím. Nova*, vol. 34, no. 6, pp. 928-932.
17. E. P. Rose and R. Shameela, (2012). "Equilibrium study of the adsorption of iron (II) ions from aqueous solution on carbons from wild jack and jambul," *Adv. Appl. Sci. Res.*, vol. 3, no. 3, pp. 1889-1894.
18. S. R. Shukla, R. S. Pai, and A. D. Shendarkar, (2006). "Adsorption of Ni (II), Zn (II) and Fe (II) on modified coir fibres," *Sep. Purif. Technol.*, vol. 47, no. 3, pp. 141-147.
19. K. U. Ahamad and M. Jawed, (2010). "Kinetics, equilibrium and breakthrough studies for Fe (II) removal by wooden charcoal: A low-cost adsorbent," *Desalination*, vol. 251, no. 1-3, pp. 137-145.
20. B. Acemioğlu, (2004). "Removal of Fe (II) ions from aqueous solution by Calabrian pine bark wastes," *Bioresour. Technol.*, vol. 93, no. 1, pp. 99-102.
21. N. Manivasakam, (2005). "Physico-chemical examination of water sewage and industrial effluents." *Phys.-Chem. Exam. Water Sew. Ind. Effl.*, no. Ed. 5.
22. U. Holzwarth and N. Gibson, (2011). "The Scherrer equation versus the 'Debye-Scherrer equation'," *Nat. Nanotechnol.*, vol. 6, no. 9, p. 534.
23. R. Balaji, S. Sasikala, and G. Muthuraman, (2014). "Removal of Iron from drinking/ground water by using agricultural Waste as Natural adsorbents," *Int. J. Eng. Innov. Technol. IJEIT Vol.*, vol. 3, pp. 43-46.
24. R. Singh, K. Kulkarni, and A. D. Kulkarni, (2011). "Application of appopolite in adsorption of heavy metals (Co and Ni) from waste water," *Chem Mater Res*, vol. 1, no. 2, pp. 16-21.
25. L. Dubey, H. K. Sharma, and R. K. Khare, (2017). "Removal of Zinc and Lead from Aqueous Solution using Low Cost Bioadsorbent *Pennisetum glaucum* (Bajara) Husk," *Adv. Bioresarch*, vol. 8, no. 4. 188-196
26. A. O. Dada, A. P. Olalekan, A. M. Olatunya, and O. Dada, (2012). "Langmuir, Freundlich, Temkin and Dubinin-Radushkevich isotherms studies of equilibrium sorption of Zn²⁺ onto phosphoric acid modified rice husk," *IOSR J. Appl. Chem.*, vol. 3, no. 1, pp. 38-45.

CITATION OF THIS ARTICLE

H K Sharma, M V Sharma, R Quadir and L Dubey. Adsorption Efficiency of Nano/Micro Cellulose for Removing Iron from Aqueous Solution and its Isotherm Studies. *Bull. Env. Pharmacol. Life Sci.*, Vol10[3] February 2021 : 85-91